When is the bait worth the risk? Modeling a compensatory ecological trap in seabirds

Authors: Cristóbal Anguita[1], Alejandro Simeone[2], Cristián F. Estades[1]

Affiliations:[1]Laboratorio de Ecología de Vida Silvestre, Facultad de Ciencias Forestales y Conservación de la Naturaleza, Universidad de Chile, Santiago, Chile

[2]Departamento de Ecología y Biodiversidad, Facultad de Ciencias de la Vida, Universidad Andrés Bello. Santiago, Chile.

Corresponding author: Cristóbal Anguita, E-mail: cristobalanguita@ug.uchile.cl

Abstract

Ecological traps occur when organisms preferentially select habitats that reduce their fitness and increase the risk of population extinction. However, habitat selection—and consequently ecological traps—can involve trade-offs between fitness components, leading to more complex and variable population responses than those predicted by previous models. Moreover, these responses are expected to differ among populations depending on how species are constrained by their life histories. A key driver that increases habitat preference and can trigger these compensatory traps is human-derived trophic subsidies. Focusing on the interaction between seabirds and fisheries, we developed a simulation model to evaluate how species with different life histories (slow, intermediate, and fast) respond to a compensatory ecological trap that reduces survival (bycatch) while increasing recruitment (trophic subsidy) across the slow-fast life history continuum. Our model reveals distinct thresholds where the benefits of trophic subsidies are outweighed by increased mortality, depending on species' life history traits. Under similar conditions, slow-lived species (e.g., albatrosses) are 1.4 times more vulnerable to extinction than intermediate species (e.g., gulls) and 4.5 times more vulnerable than fast-lived species (e.g., cormorants), which show greater resilience and greater potential for population growth. These findings highlight that fisheries are selectively filtering life history strategies, disproportionately affecting slow-lived species while favoring fast-lived ones. Our results extend previous predictions about ecological traps and underscore the need to account for a wider range of fitness trade-offs. We propose that ecological traps offer a crucial theoretical framework for understanding and managing interactions between wildlife and human-derived trophic subsidies, such as those involving seabirds and fisheries.

Keywords: trophic subsidy, discards, bycatch, life-history, fisheries

Highlights:

- Ecological traps may involve trade-offs between fitness components.
- Compensatory traps can generate nonlinear population responses.
- Compensatory traps may filter life history strategies, favoring fast-lived species.
- Expanding the trap framework is key to improving management initiatives.

1. Introduction

A common assumption in ecology is that an organism's ability to survive and reproduce is closely linked to its habitat preferences, which have been shaped by natural selection. However, organisms do not always make adaptive choices and may instead prefer habitats that reduce their fitness—a phenomenon known as 'ecological traps' (Dwernychuk and Boag, 1972; Gates and Gysel, 1978). Theoretical studies have shown that traps heighten the risk of extinction for local populations and spatially structured metapopulations (Delibes et al., 2001; Donovan and Thompson, 2001; Fletcher et al., 2012a; Hale et al., 2015; Kokko and Sutherland, 2001; Kristan et al., 2003). Empirical evidence further indicates that ecological traps are widespread in terrestrial and marine ecosystems and frequently result from rapid, human-driven environmental changes that outpace species' adaptive responses (Hale and Swearer, 2016; Robertson et al., 2013; Swearer et al., 2021). As these changes persist, ecological traps are likely to become more frequent in the future.

Previous theoretical models of traps commonly assume maladaptive habitat selection in relation to survival or reproduction (Delibes et al., 2001; Donovan and Thompson, 2001; Fletcher et al., 2012b; Hale et al., 2015; Kokko and Sutherland, 2001; Kristan et al., 2003). However, ecological traps may involve trade-offs between different fitness components, whereby seemingly maladaptive behavior concerning survival (or reproduction) may be offset by enhanced reproduction (or survival) (Battin, 2004). Furthermore, ecological and evolutionary responses to these fitness trade-offs are expected to be influenced by species' life histories, particularly their position along the slow-fast continuum (Saether, 1987; Stearns, 1992). Species with a slower pace of life—characterized by longer lifespans, lower reproductive potential, and reduced maximum population growth rates—are anticipated to be more vulnerable to local extirpation due to ecological traps (Hale et al., 2015; Kokko and Sutherland, 2001). However, the introduction of traps involving demographic trade-offs and their interactions with

life-history traits may lead to outcomes different from those predicted by previous models, both within populations and between species. This could potentially result in nonlinear responses, multiple equilibria, and even population growth, as well as contrasting responses along the slow-fast continuum (Clark and Luis, 2020; Herrando-Pèrez et al., 2012; Munch et al., 2005; Sæther et al., 2004). Therefore, understanding the specific mechanisms through which traps influence life histories is critical for preventing and effectively managing their consequences on populations (Robertson and Blumstein, 2019; Swearer et al., 2021).

Compensatory traps may arise from predictable anthropogenic food subsidies (Grémillet et al., 2008). In these scenarios, the enhancement of individual fitness due to subsidies may be offset by heightened risks of mortality, such as pollution, competition, predation, or accidental death. For instance, seabirds attracted to fishing vessels for trophic subsidies—including bait, catches, and discards—face the risk of accidental death (bycatch) through entanglement, collisions, or hooking (Abraham et al., 2009; Pierre et al., 2012; Zhou et al., 2019; Zhou and Brothers, 2022). Recently, bycatch has been identified as the primary threat to seabirds at sea, driving population declines and heightening extinction risk (Dias et al., 2019; Richards et al., 2024, 2021).

Conversely, food provided by fisheries—primarily through discards (Bicknell et al., 2013; Garthe et al., 1996; Sherley et al., 2019; Votier et al., 2004)—has the potential to mitigate bycatch mortality, leading to improved breeding success and population recruitment (Cleeland et al., 2021; Genovart et al., 2016; Pardo et al., 2017; Rolland et al., 2010, 2009, 2008). This compensatory effect is expected to be more pronounced in fast-lived species due to their higher demographic sensitivity to reproduction compared to slow-lived species, which are more sensitive to survival (Heppell et al., 2000; Saether and Bakke, 2000). However, the extent to which these compensatory effects are influenced by life history traits remains an open question (Genovart et al., 2017). Additionally, the ecological trap framework has

been underutilized in explaining and predicting seabird-fisheries interactions and has not been applied to other large marine vertebrates affected by fisheries, including sea turtles, mammals, and elasmobranchs (Lewison et al., 2014). Furthermore, ecological traps remain relatively understudied in marine ecosystems (Swearer et al., 2021).

We build upon the above case study to better understand and predict the consequences of compensatory ecological traps along the slow-fast continuum of life history of seabirds. Specifically, we introduce a spatially explicit, individual-based model (IBM)(Grimm and Railsback, 2005) to evaluate how species with different life histories (slow, intermediate, and fast) respond to a compensatory ecological trap. This trap involves a demographic trade-off between reduced survival due to bycatch and increased recruitment—both breeders and fledglings—driven by trophic subsidies from fishery discards. We also discuss the model's assumptions, predictions, and implications for seabird management and conservation.

2. Methods

2.1. The model

The description of the model follows the protocol created by (Grimm et al., 2006) to explain IBM within an ecological framework. Following the description of the model, we explain the experiments conducted in detail. The model was developed in R (R Core Team, 2023) using the NetLogoR (Bauduin et al., 2019), dplyr (Wickham et al., 2023), and data.table (Barrett et al., 2024) packages.

2.2. Model Purpose

The model aims to simulate population responses of species with varying life-history strategies along the slow-fast continuum under compensatory ecological trap scenarios. In our simulation, the compensatory trap is established by introducing additional energy to a limited area of the habitat while

simultaneously increasing mortality risk within the same region. This enhanced habitat improves foraging efficiency (reducing movement costs) and recruitment (breeding success and fledging), but the elevated mortality risk depends on specific trap parameters. The base model is a spatially explicit simulation of the life cycle of a colonial bird. It integrates life-history traits, memory-based foraging behaviors, reproduction, and mortality in a patchy, energy-limited environment that changes dynamically as energy is consumed over time.

2.3. Entities, state variables, and scales

The model consists of four entities: (1) the population and its associated attributes, (2) an energy raster representing the environment and its attributes, (3) the colony, and (4) the trap raster and its associated attributes. Each individual in the population is defined by five key state variables: identity code, spatial coordinates (both current and from the previous step), age, breeding state, and energy. The identity code is a unique identifier assigned to each individual at the start of the simulation or upon birth. Spatial coordinates represent the individual's position on the raster map, defined by the row and column numbers. The age of individuals ranges from zero (individuals less than one year old) to the maximum lifespan, which is determined by the life history traits of the species. The breeding-state variable includes three categories: non-breeder, breeder, and chick. Energy (E) represents the energetic state of non-breeding and breeding individuals, and it is governed by the following dynamic equation:

$$E^{(t)} = E^{(t-1)} + C - B - A - R,$$

where C represents the energy consumption from foraging, B is the fixed energy lost through basal metabolism (denoted as β_basal), M is the energy expended through movement (calculated as β_loss × movement distance), and R is the energy allocated to reproduction. The reproductive energy (R) includes the constant energy required for offspring production and its supply throughout the breeding

season (denoted as β_supply). For simplicity, chick energy expenditure is not modeled explicitly. Fledging probability is determined by parental provisioning, as described in the Reproduction sub-model.

The energy raster representation of the environment consists of a 21 × 21 grid, arranged with a toroidal (donut-shaped) topology. This means that when an individual crosses the grid's boundary, it reappears at the opposite edge, avoiding potential artifacts due to spurious edge effects. Each cell in the grid is assigned an energy value, expressed in kilojoules (KJ), and the cell's position is defined by its column and row numbers. Energy values are drawn from a zero-inflated negative binomial distribution (ZINBI) (Stasinopoulos and Rigby, 2023), providing variability in the energy content across the grid. The colony is positioned at the center of the grid, with coordinates (xcord, ycord) = (10,10). The trap raster is defined by the presence or absence of a trap in each cell, with its layout also determined by the grid's column and row coordinates.

A year is represented as 365 days in the model, with each simulation step corresponding to 6 hours. As such, each day is composed of 4 steps, and a full year consists of 1460 steps. The model does not incorporate a circadian rhythm but includes seasonality, with distinct breeding and non-breeding periods. The breeding period is divided into two phases: the 'laying window,' during which individuals produce offspring within the colony, and the 'fledging period,' in which parents commute between the sea and the colony to feed their chicks until they fledge or die. In our model, we represent a typical seabird phenology, with a breeding period lasting 146 days. This includes a 20-day 'laying window' for egg-laying and a 126-day 'fledging period,' which is consistent with the mean lengths of the incubation and fledging periods observed in seabird species (Schreiber and Burger, 2001).

2.4. Process overview and scheduling

The general schedule of the program is described in Fig. 1. The program begins by defining the initial conditions, including the collection of individuals, their memory, and their state variables, the environment (energy raster), and the trap scenario. Afterward, the model begins to operate. Within each time step (6 hours), seven main sub-models or modules are processed in the following order: (1) Energy replenishment, (2) Movement, (3) Trap mortality, (4) Reproduction, (5) Mortalities, (6) Updates and (7) End simulation.

In the Energy Replenishment module, the energy of the environment and the subsidy are replenished (see Energy Replenishment module). Next, the Movement and Foraging sub-model operates, and birds rest, feed (consume energy), or move (random walk or 'oriented' random walk) based on their hunger level (i.e., energy level, see 'Movement and Foraging' sub-model). In the Trap Mortality module, deaths due to trap interactions are evaluated. Following this, the Reproduction sub-model operates. Satiated non-breeders who meet the breeding conditions during the laying window will go to the colony and produce offspring (see 'Reproduction' sub-model). During the fledging period, satiated breeders return to the colony to feed their chicks and will continue to do so until the chick fledges or dies (see 'Reproduction' sub-model). In both cases, once this occurs, the breeders transition to non-breeder status. The same applies at the end of the fledging period for unsuccessful breeders (those whose chicks did not fledge). Next, the Mortalities sub-model operates, and death probabilities are assessed due to starvation, age, and other constant mortality factors (see 'Mortalities' sub-model). At the end of the algorithm, the age, energy, and memory of individuals are updated. The basal energy expenditure (β_basal) and the energy lost due to movement ($\beta\_loss \times$ movement distance) are subtracted from the individuals' energy reserves.

The memory is then updated to store the coordinates and respective foraging success of each individual's current cell. Subsequently, for each individual, the cells in their memory are arranged from

highest to lowest foraging success, and the first n = β_memory cells are stored. Individuals retain their memory throughout their lifetime. Lastly, the simulation stops either when the last iteration is reached or if the population becomes extinct. In both cases, the program saves the output.

2.5. Design concepts

2.5.1. Basic principles

This model is built on the assumption that seabird populations are food-limited and energetically enriched habitats (trophic subsidies) generate benefits for foraging and reproduction, but they also increase the risk of mortality. Consequently, population vital rates respond in opposite directions to habitat selection. The model is based on animals' ability to make behavioral and reproductive decisions using their previous foraging experience and current condition (energy). For instance, birds decide when to leave their present patch, in which direction to move, or when to go to reproduce in the colony.

2.5.2. Emergence

Population size emerges as the result of individuals' foraging success, survival, and reproduction within a patchy and dynamic environment with limited resources. Movement is guided by a combination of experience and randomness. Reproduction is influenced by probabilities weighted by foraging success and life history traits. Mortality rates are determined by the combination of foraging success, age-specific mortality curves, and interactions with the environment (including trap mortality). As such, population growth is not directly modeled but emerges from the interplay of these factors within the simulation

2.5.3. Adaptation

Individuals follow spatially explicit movement rules, guided by their hunger (energy level) and previous foraging experience, to locate food patches.

2.5.4. Learning

Individuals remember the locations of previously visited cells and the duration of successful foraging there (foraging success is defined as the cumulative time spent in a cell where consumption exceeds 95% of the maximum possible consumption, i.e., βhunger). As individuals age, they accumulate foraging experience and, on average, spend more time in higher-quality patches. Individuals do not learn from others' experiences, relying solely on their own interactions with the environment.

2.5.5. Prediction

Individuals determine their movement direction based on the quality of habitats where they have previously foraged. These decisions are made without estimating future conditions or the consequences of their actions. As a result, individuals rely solely on past experiences to guide their foraging behavior

2.5.6. Sensing

Individuals know their present location, energy level, and memory. Based on these traits and seasonality, they can modify their behavior (as explained in the sub-model section). Individuals do not identify the habitat of their neighboring cells, nor do they recognize emergent properties of the population, such as its size (whether at sea or in the colony).

2.5.7. Interaction

The model simulates an environment with limited energy, where exploitation competition is the primary form of indirect interaction. There are no hierarchical structures governing habitat selection or food consumption among individuals. Additionally, individuals do not assess the number of others in

the same cell, nor can they predict the potential future locations of other individuals, which may influence their movement decisions.

2.5.8. Stochasticity

Randomness in the model is incorporated through probabilities in individual movement decisions, reproduction, mortality, and energy renewal from the environment. Individuals without foraging experience follow a random walk pattern. Birds with prior experience in high-quality cells use weighted probabilities, based on their experience, to move towards those areas rather than following a straight-line path. Reproduction events (both laying and fledging) and mortality events (age-related, trap-related, starvation, and constant mortalities) are determined by weighted probabilities. The energy content of each cell changes dynamically over time, adding an additional layer of unpredictability.

2.5.9. Collectives

Individuals do not form or belong to aggregations that influence each other's behavior or decisions. Each individual's actions are independent of others, and there are no social dynamics affecting habitat choice, foraging, or reproduction.

2.5.10. Observation

At the end of each simulation, population-level variables were recorded, including total population size, number of newborns, recruits (breeders and chicks), and deaths, categorized by cause.

2.6. Initialization

Prior to each simulation, 180 individuals were randomly distributed across the environment, all assigned a non-breeding status. The ages of individuals were randomly drawn from the age distribution of populations under stationary growth conditions (90–100 years in control conditions) for each life-

history type, based on prior model runs. The individuals' energy levels followed a normal distribution with a mean of β_hunger ± 10 SD. At the beginning of the simulation, individuals had an 'empty' memory. The energy content of each cell was randomly sampled from a ZINBI distribution and scaled by the parameter β_food to reach the desired population size. The spatial configuration of the trap was defined by the corresponding trap parameters (Table 1).

2.7. Sub models

This section provides a detailed description of the sub-models for Energy Replenishment, Movement and Foraging, Trap Mortality, Reproduction, and Mortalities.

2.7.1. Energy replenishment sub-model

When the energy of a cell decreases to a minimum value due to consumption by individuals, it begins to increase proportionally to its initial value (Energy initial[i,j]) according to a logistic function:

$$\text{Energy}[i,j] = \text{Energy initial}[i,j] \times \text{Prop(replenishment)}[i,j];$$

where,

$$\text{Prop(replenishment)[i,j]} = \frac{1}{1 + e^{k(\text{replenishment steps[i,j]} - \beta\_\text{replenishment})}},$$

Where replenishment steps[i,j], is the number of time steps elapsed since energy replenishment began for cell [I, j], β_replenishment is the x value of the function's midpoint and k is the steepness of the curve (k = 1). In this module, the energy from the subsidy (β_subsidy) is subsequently added to the cells where the trap is located. The amount of energy added depends on the trap parameters defined in the experiment (see Table 2).

2.7.2. Movement and Foraging sub-Model

This sub-model simulates the movement and foraging behavior of individuals within a one-step period (6 hours), considering their energy levels and decision-making processes. During each simulation step, birds either rest, feed, or move, depending on their hunger level. If a bird is not hungry (energy > β_hunger), it remains in the same location and rests. If it is hungry (energy < β_hunger), it attempts to consume energy in its current location. Energy consumption is modeled using a two-parameter Holling Type II response (Holling, 1959), commonly applied to approximate feeding behaviors observed in nature (Sibly et al., 2013). The relationship is expressed as:

$$\text{Consumption} = \beta\_\text{hunger} * \frac{\text{energy[i,j]}}{\text{energy[i,j]} + \beta\_\text{holling}}$$

Where β_hunger represents the maximum energy consumption in kilojoules (KJ), energy[i,j] is the available energy in the individual's current cell, and β_holling is a constant that determines the rate at which energy consumption approaches its maximum as available energy increases. Energy consumption by individuals in the same cell occurs sequentially (using a for-loop) and in random order, with no hierarchical structure among individuals. Following the marginal value theorem, individuals leave the current cell when their consumption drops below a certain threshold (Charnov, 1976). In contrast to the marginal value theorem, which defines this threshold relative to the habitat, our model assumes that individuals base this decision on their own energetic state. Specifically, they leave the current cell when the energy they consume falls below or equals their basal energy expenditure (parameter β_basal).

For modeling movement, birds follow a memory-biased random walk, directing their movement toward previously successful foraging locations. The only exception is recruits leaving the colony, which lack prior experience and thus follow an unbiased random walk. These naïve birds move to a neighboring cell within their movement radius (β_radius), following a modified random walk pattern in

which diagonal movement is penalized by a factor of 0.7 to maintain an isotropic movement pattern. For all other birds (i.e., those with at least one memory cell), movement is biased toward the cell where they had the greatest foraging success. In these cases, the probability of moving to a given cell within their movement radius is determined by a logistic function that regulates the degree of directional stochasticity (based on k_dire and β_dire parameters, see Figure S1). This approach allows birds to be guided toward their preferred cell while permitting deviations from a straight-line trajectory (see Figure S2).

2.7.3. Trap-mortality sub-model

In this module, the probability of mortality for individuals located in trap cells (trap raster) is assessed. The trap lethality parameter (β_lethality) is compared to a random sample drawn from a uniform distribution between 0 and 1 (U). The probability of mortality for an individual is then expressed as:

$$[\text{Trap Mortality}] = \begin{cases} 1, & \text{if } \beta\_\text{lethality} > U \\ 0, & \text{otherwise} \end{cases},$$

and mortality occurs (with a probability of 1) when the lethality parameter exceeds the value of U; otherwise, the probability is zero. The meaning of U remains consistent throughout the following sections.

2.7.4. Reproduction sub-model

This sub-model simulates the reproduction process of seabirds during the breeding season, including chick production during the 'laying window', provisioning by the parents, and the fledging of chicks. For simplicity, the model treats birds as asexual organisms. Reproduction depends on the age of first reproduction (β_firstbreed) and the individual's current (β_hunger) and wintering

(β_reproduction) energetic condition. The wintering condition is determined by a logistic function based on the number of steps in which individuals were satiated during the non-breeding period:

$$[successful\ winter] = \begin{cases} 1, & if\ \frac{1}{1 + e^{k(satiated\ steps - \beta\_reproduction)}} > U \\ 0, & otherwise \end{cases},$$

where β_reproduction is the *x* value of the function's midpoint and *k* the steepness of the curve (k=1).

During the 'laying window,' a bird can reproduce if its energy and age exceed certain thresholds (energy > β_hunger, age ≥ β_firstbreed), and if it had a successful winter (successful winter = 1). If these conditions are met, the bird moves to the colony in a straight line over one time step and produces n=β_clutch number of chicks. When reproduction occurs, the 'mother' loses a fixed amount of energy (β_supply), and the chick(s) gain the same amount of energy (β_supply).

During the 'fledging period,' chick provisioning is based on the hunger parameter (β_hunger). Once satiated, the breeder returns to the colony in a straight line over one time step, regardless of their location, to supply the chicks. For simplicity, the model does not explicitly simulate the various activities of birds during the reproductive stages, such as incubation, brood-guarding, or creches. Chicks are fed a fixed amount of energy throughout the reproductive stage, equivalent to the supply parameter (β_supply), while the 'mother' loses a constant amount of energy (β_supply). The fledging of the chicks is a probabilistic event, determined by a logistic function of the number of times the chick was fed by its mother:

$$[fledging] = \begin{cases} 1, & if\ \frac{1}{1 + e^{k(provisioning\ events - \beta\_fledge)}} > U \\ 0, & otherwise \end{cases},$$

where β_fledge represents the x-value of the function's midpoint, and k indicates the steepness of the curve (k = 1). Fledging occurs when the probability reaches 1, at which point chicks transition to non-breeders, and their energy is set to the hunger parameter (β_hunger).

2.7.5. Mortalities sub-model

In this module non-trap related mortalities are evaluated, including starvation, age-dependent, and constant mortalities.

Starvation mortality: The probability of mortality due to starvation is assessed at each time step. It is determined by a logistic function based on the accumulated number of days an individual has spent without consuming energy from foraging or, in the case of chicks, without being provisioned by the parent.

$$[Starvation\ mortality] = \begin{cases} 1, & if\ \frac{1}{1 + e^{k(starving\ steps - \beta\_starvation)}} > U \\ 0, & otherwise \end{cases},$$

where β_starvation is the *x* value of the function's midpoint and *k* the steepness of the curve (k=1).

Age-dependent mortality: The probability of mortality due to age is assessed every five days and is estimated using a three-parameter exponential decay function based on the individual's age.:

$$[\text{Age} - \text{dependent mortality}] = \begin{cases} 1, & \text{if } [\beta\_\min + (\beta\_\max - \beta\_\min)e^{\frac{-\text{age}}{\beta\_\text{decay}}}] > \text{U} \\ 0, & \text{otherwise} \end{cases},$$

where β_min is the minimum mortality rate, β_max is the maximum mortality rate, and β_decay is the constant rate of decay. By varying the parameters β_min and β_max, we assign age-dependent mortality curves for each life history (with the same decay rate, β_decay = 5, as detailed in the supplemental material). Additionally, individuals die when they reach the maximum age (β_senescence) specific to their life history.

Constant mortality: This is a fixed probability of death, assessed once per year during the first step of each year:

$$[\text{Constant mortality}] = \begin{cases} 1, & \text{if } \beta\_\text{constant} > U \\ 0, & \text{otherwise} \end{cases}$$

2.8. Calibration and parameterization

The parameters used in the model are presented in Table 1. We calibrated the parameters as follows: First, we set the basal expenditure parameter (β_basal) according to the average ratio between the field metabolic rate (FMR) and the basal metabolic rate (BMR) in seabirds, i.e., β_hunger/3.5 (Schreiber and Burger, 2001). Subsequently, we calibrated the β_hunger parameter so that, during the non-breeding season, individuals consumed an amount equivalent to the FMR of an average seabird.

Considering the energy replenishment parameter, individuals fed most frequently 1 or 2 times per day and consumed an average of 1200 KJ per day. Seabirds tend to increase their FMR throughout the breeding season, from incubation to brood to creche (Dunn et al., 2018). Accordingly, the parameter for energy loss from movement (β_loss) was calibrated so that birds increased their average daily consumption by approximately 40% during the breeding season (~1600 KJ/day), due to the cost of commuting between the colony and the foraging grounds.

The movement radius was calibrated to allow individuals to reach the "edge" of the environment—used as a reference point in the toroidal landscape—within one day (four steps). The parameters regulating movement stochasticity (k_dire and β_dire, Table 1) were adjusted to balance randomness in movement while minimizing the risk of frequent starvation-related mortality (see, Figure S1, S2).

We set the Holling type 2 constant (β_holling) so that the function reaches half of its maximum value when the energy available to an individual equals the maximum consumption (i.e., β_hunger). The parameter for the energy cost of chick production and chick supply (β_supply) was established at 10% of the β_hunger parameter. This represents an intermediate cost, considering that for most of the

nestling period, seabird parents deliver meals weighing 5 to 35% of the adult body mass (Schreiber and Burger, 2001).

Based on the parameters described above, chicks were fed most frequently one to two times per day. This feeding frequency falls within the range typical for seabirds provisioning their chicks, with variations ranging from several meals a day to one every one or two days. Consequently, we adjusted the fledging parameter to ensure that chicks fed at least once a day had a high probability of fledging. The parameter for starvation mortality was determined based on the allometric starvation model for an average seabird, following the approach of (Peters, 1983).

We calibrated the energy distribution parameters of the raster (ZINBI distribution, β_mu, β_sigma, β_nu) to achieve a high degree of patchiness while minimizing frequent deaths among individuals under control conditions (see above). The selected distribution included 40% zeros and ranged from 0 to 12 units (KJ).

We parameterized three life histories—slow, intermediate, and fast—based on typical reproduction and survival traits in seabirds following Schreiber and Burger, (2001), including clutch size, age at first reproduction, age-specific mortality, and senescence. As a reference, we used the parameters of an average albatross for the slow species, a seagull for the intermediate species, and a cormorant for the fast species (Table 1).

2.9. Experiments

The base scenario featured a compensatory trap in the highest-quality habitat, with energy levels above the 9th quantile. Such scenarios are common in marine predator-fishery interactions, as both predators and fisheries tend to co-occur in highly productive areas, including mesoscale frontal systems, eddies, upwelling zones, and continental shelves (Karpouzi et al., 2007; Scales et al., 2018;

Welch et al., 2024). The trap occupied 15% of the habitat, was present year-round, and added a daily subsidy to the environment. Simulations ran over a 100-year period, beginning with a 24-year initial phase during which populations were allowed to reach stable equilibrium (the 'control condition'). On the year 25, the compensatory trap began operating. We defined three levels for both mortality and subsidy—small, medium, and large. Preliminary analyses of population responses to a mortality gradient revealed that life histories tend to converge at both extremes of mortality. Therefore, we set intermediate, realistic values (with realized mortality ranging from 2% to 23%) where the differences among life histories were more pronounced (Table 1). We defined subsidy levels at which populations reached 1, 2, and 3 times the carrying capacity under control conditions without trap mortality. Combining the three factors (mortality, subsidy, and life-history) at each level produced a total of nine simulation scenarios, with seven replicates per scenario.

Given the distinct life histories of the species and the sources of stochasticity, populations reached different equilibrium sizes (slow < intermediate < fast). Therefore, for each replicate across the nine scenarios, we standardized population sizes by their average equilibrium sizes under control conditions. Finally, we analyzed both short-term and long-term population responses to compensatory traps. Short-term response was measured as the average standardized population size during the first 10 years after the trap's introduction, while long-term response was measured as the average standardized population size over the last 10 years of the simulation.

Additionally, we modified the base scenario to include three variations: (1) a larger-area scenario, with the trap covering 25% of the habitat; (2) a smaller-area scenario, covering 5% of the habitat; and (3) a scenario in which the trap occurred randomly throughout the habitat. In these scenarios, we analyzed only the long-term differences compared to the base model. Results are expressed as the mean with one standard deviation (SD), unless otherwise specified.

3. Results

3.1. Base trap scenario

Slow Species (e.g., albatross): At low mortality, the slow species maintained a population size similar to the control under low subsidy (Figure 3a) and exhibited slight growth at medium (1.1 ± 0.14 times control) and high subsidy (1.1 ± 0.09 times control) levels in the short term (Figure 3a-c). However, in the long term, the population declined as subsidy levels increased (Figure 3a-c), reaching 0.3 ± 0.09 times the control population under high subsidy (Figure 3c). At medium mortality, the slow species experienced a more pronounced short-term decline, which intensified with higher subsidy levels (from 0.86 ± 0.05 times control at low subsidy to 0.76 ± 0.1 times control at high subsidy, Figure 3d-f). Ultimately, this led to extinction across all subsidy levels in the long term (100% probability, Figure 3d-f). Under high mortality, the slow species showed an even steeper short-term decline as subsidy levels increased, resulting in a 100% probability of extinction (Figure 3g-i).

Intermediate Species (e.g., gull): At low mortality, the intermediate species achieved slightly higher asymptotic growth than the control in the long term (1.1 ± 0.02 times control, Figure 3a). At medium and high subsidy levels, it attained more substantial asymptotic growth, reaching 1.7 ± 0.09 and 2.6 ± 0.1 times the control, respectively (Figure 3b-c). Under medium mortality, the intermediate species exhibited a non-linear short-term response, peaking at medium subsidy levels (1.1 ± 0.12 times control, Figure 3e-f). However, in the long term, it showed lower asymptotic growth than the control at low subsidy (0.7 ± 0.19 times control, Figure 3d) and faced a tendency toward decline and eventual extinction at intermediate and high subsidy levels, with 43% and 71% probabilities of extinction, respectively (Figure 3e-f). Under high mortality, the intermediate species experienced sharp short-term declines and ultimately reached a 100% probability of extinction in the long term (Figure 3g-i).

Fast Species (e.g., cormorant): At low mortality, the fast species grew rapidly in the short term and reached asymptotic growth in the long term, attaining 1.3 ± 0.05, 1.8 ± 0.04, and 2.7 ± 0.09 times the control size as subsidy levels increased from low to high (Figure 3a-c). Under medium mortality, the fast species exhibited a non-linear short-term response similar to that of the intermediate species, with its highest population size observed at medium subsidy (1.4 ± 0.09 times control, Figure 3d-f). In the long term, it reached asymptotic growth at 1.2 ± 0.06 and 1.6 ± 0.16 times the control as subsidy levels increased from low to medium. At high subsidy, it grew to a larger size, but without reaching asymptotic growth (2.3 ± 0.28 times control, Figure 3f). Under high mortality, the fast species initially matched control population sizes at low and medium subsidy levels but experienced a short-term decline at high subsidy (0.8 ± 0.11 times control, Figure 3g-i). In the long term, it stabilized at sizes similar to the control under low subsidy (0.9 ± 0.11 times control, Figure 3g), while the likelihood of decline increased at medium and high subsidy levels, reaching 29% and 100% probabilities of extinction, respectively (Figure 3h-i).

3.2. Trap variations

The smaller-area trap increased the resilience of declining populations compared to the base model and reduced the carrying capacity (K) for growing populations (Figure 1S). In contrast, the larger-area trap generally had more severe impacts on declining populations and increased K for growing populations compared to the base model (Figure 1S). Overall, the random trap scenario was less severe for declining populations and also increased K for growing populations in comparison to the base model (Figure 1S).

4. Discussion

Understanding the mechanisms behind ecological traps is essential, especially given the rapid, human-induced environmental changes that present poorly known risks to populations. Previous ecological trap models have generally assumed reduced survival and/or reproduction among trapped populations (Battin, 2004), leading to the conclusion that these traps inevitably decrease population sizes and heighten vulnerability to stochastic extinction. Our model introduces a novel trade-off: increased recruitment—driven by trophic subsidies—counterbalanced by a reduction in survival rates. While the model predicts similar results to previous models, it also reveals critical differences. As expected, the severity of trap impacts increases when traps occupy larger portions of available habitats or when they emerge in higher-quality habitats that attract greater preference (Delibes et al., 2001; Fletcher et al., 2012b; Hale et al., 2015). Below, we explore novel aspects of our model predictions, the assumptions underpinning them, areas for future refinement, and contrasts with existing evidence of seabird-fishery interactions. Finally, we discuss their implications for effective management and conservation strategies.

4.1. Fitness trade-offs within the ecological trap framework

Our model revealed a critical interaction between trophic subsidies and mortality, resulting in more complex population responses than anticipated by previous ecological trap models. These included non-linear responses both over time and across different levels of subsidy and mortality. All three life histories displayed non-linear temporal dynamics, where the initial positive effects of recruitment (breeders and fledging, Figure S3, S4) outweighed mortality (Figure S5). However, populations were unable to sustain growth in the long term, leading to eventual declines (e.g., the slow-lived species in scenario C, the intermediate-lived species in scenario E, and the fast-lived species in scenario G, Figure 2). This highlights the challenge of detecting a trap that appears advantageous in the short term but can lead to long-term population extinction. Overall, these responses are expected to be more common

in fast-lived species, as they have greater potential for population growth, which also implies more pronounced density dependence (Herrando-Pèrez et al., 2012), higher demographic stochasticity (Sæther et al., 2004) and a greater tendency toward nonlinear and chaotic dynamics (Clark and Luis, 2020; Rogers et al., 2022).

Similarly, all three life histories exhibited non-linear responses across varying levels of mortality and subsidy. At lower mortality levels, trophic subsidies effectively compensated for mortality and promoted population growth. However, once mortality exceeded a critical threshold, subsidies amplified mortality impacts—specifically, increased habitat preference elevated effective mortality (Figure S5)—ultimately causing population declines and, in some cases, extinction. In contrast, simulations by Hale et al., (2015) showed that reductions in either fecundity or survival within traps individually decreased metapopulation persistence, but their combined effects did not further amplify trap impacts. Our findings emphasize the importance of incorporating trade-offs among fitness components into ecological trap frameworks (Battin, 2004), as habitat preference can cause fitness components to respond antagonistically or synergistically, resulting in more diverse responses than those anticipated by ecological trap models.

4.2. Influence of life history on compensatory ecological traps

Additionally, our results demonstrate that the interplay between mortality and subsidies is heavily influenced by species' life history traits along the slow-fast continuum (Saether, 1987)—the main axis of life history variation across several taxa, including mammals, birds, reptiles, fishes, insects, and plants (Capdevila et al., 2020; Cooney et al., 2020; Gaillard et al., 2016; Sibly et al., 2012). Considering the three habitat preference scenarios (base, higher, and lower area), our model predicts that the species with the slowest life history is 1.41 and 4.5 times more likely to face extinction

compared to species with intermediate and fast life histories, respectively. These findings align with theoretical expectations, highlighting that 'slow' life-history species are particularly vulnerable to local extirpations caused by traps (Hale et al., 2015). In contrast, faster species exhibit greater resilience and, under similar conditions, can thrive, with population sizes potentially increasing up to threefold compared to control groups. These results suggest that compensatory traps may amplify the selective filtering of life history more intensely than previously anticipated (Hale et al., 2015; Kokko and Sutherland, 2001).

Recent studies within a broader context agree with our findings, indicating that species with longer generation times require extended recovery periods following disturbances, while species with shorter generation times tend to exhibit greater resilience (Capdevila et al., 2022). Furthermore, animals with slower life histories are generally at greater risk of extinction compared to faster-reproducing species, including plants, mammals, birds, reptiles, amphibians, and freshwater fish. This could result in big shifts in ecological strategies across the tree of life (Carmona et al., 2021; Cooke et al., 2019; Richards et al., 2024, 2021). Integrating various trade-offs between fitness components into the theoretical framework of ecological traps is thus essential for identifying traps and clarifying their contribution to the global filtering of animal life histories.

4.3. The case of seabirds-fisheries interaction

Model predictions agree with previous research documenting a variety of responses in seabirds across the slow-fast continuum in relation to fisheries discards and bycatch. For instance, studies on slow species such as albatross and shearwater suggest that while fisheries subsidies can enhance reproductive traits like recruitment and breeding success, these gains are offset by reduced survival rates due to bycatch, ultimately causing important population declines (Cleeland et al., 2021; Genovart

et al., 2017, 2016; Pardo et al., 2017; Rolland et al., 2010, 2009, 2008; Tuck et al., 2015; Véran et al., 2007). A well-documented case in South Georgia illustrates the impact of bycatch on the wandering (*Diomedea exulans*), gray-headed (*Thalassarche chrysostoma*), and black-browed (*Thalassarche melanophris*) albatrosses. Despite potential reproductive and recruitment increases from fishery discards, bycatch has led to drastic declines in these populations, estimated at 40–60% over the past 35 years (Pardo et al., 2017). Similarly, the Balearic shearwater (*Puffinus mauretanicus*), Europe's most endangered seabird, has experienced substantial population declines due to bycatch. Projections suggest that, if bycatch rates remain unchanged, this species could face extinction within the next 61 years (Genovart et al., 2016). These findings are reinforced by recent studies that seabird life history traits predict extinction risk and vulnerability to anthropogenic threats, including bycatch (Richards et al., 2024, 2021).

In contrast, for species with fast life history traits our model predicts greater resilience and even potential for population growth in response to compensatory traps. Discards can positively influence various reproductive traits of faster seabirds (Oro et al., 2013), which often demonstrate greater phenotypic plasticity in reproduction compared to slower species. These species, which lay up to six eggs (Schreiber and Burger, 2001), show earlier laying dates, increased clutch sizes, and improved hatching and breeding success. Notable examples include Audouin's gull (*Larus audouinii*), the Yellow-legged gull (*Larus cachinnans*), and the Lesser Black-backed gull (*Larus fuscus*) (Oro, 1996; Oro et al., 1996, 1995). Studies have shown a positive correlation between subsidy availability and population size, as well as a negative correlation with population variability in these gull species. This suggests that subsidies can mitigate the high demographic stochasticity inherent to fast life histories (Oro et al., 2013). Surprisingly, evidence for the positive effects of fishery discards on seabird population sizes remains largely circumstantial. Most such evidence stems from Northern Hemisphere seabirds,

including black-backed gulls (*Larus marinus*), herring gulls (*Larus argentatus*), great skuas (*Stercorarius skua*), northern gannets (*Morus bassanus*), and northern fulmars (*Fulmarus glacialis*). These species experienced rapid population growth during the peak of discard production in the 20th century but have since stabilized or declined (Bicknell et al., 2013; Langlois Lopez et al., 2023; Oro et al., 2013; Wilhelm et al., 2016). While current fishery discards are approximately half of 1980s and 1990s levels, recent estimates suggest that global fisheries still discard between 7 and 16 million tons annually, with nearly 60% originating from trawl fisheries (Gilman et al., 2020). This substantial volume of discards likely continues to sustain large seabird populations. For instance, one extensive study found that despite a 48% decrease in North Sea discards from 1990 to 2010, these discards still supported an estimated 3.3 to 9.7 million seabirds annually (Sherley et al., 2019). These findings highlight the urgent need to reduce uncertainties surrounding global discard estimates and to investigate their role in driving compensatory traps for seabirds.

4.4. Model assumptions, caveats, and future improvements

Our model was based on two key assumptions. First, we assumed that populations were energetically limited. Second, we assumed that species with different life histories were approximately bioequivalent, meaning that they acquire and use energy in the same way, sharing all parameters except for life history. This assumption meets with the "energy equivalence rule," a central principle of the metabolic theory of ecology (Brown, 2004; Robert Burger et al., 2021), which posits that energy partitioning among species in space is independent of body mass, due to compensatory variation in metabolism-mass and abundance-mass relationships (Hatton et al., 2019). However, evidence from birds suggests that “population metabolism” (i.e., the total amount of basal energy used by a population per unit area) tends to be higher in larger species (Hatton et al., 2019), implying that compensatory effects may be smaller for slower species than predicted by our model. Nevertheless, if

the assumption of bioequivalence does not hold, compensatory traps could lead to population responses that are difficult to predict. Such responses might include changes in habitat use, vital rates, population growth rates, and overall population sizes.

Additionally, to simplify our model, we assumed identical reproductive phenology across life histories. This assumption allowed us to evaluate traps with equal exposure for all life histories, but it may overlook critical aspects of life-history variation. For example, the duration of the developmental period is a fundamental axis of life-history variation (Cooney et al., 2020). Differences in developmental times, and consequently in the use of parental habitat, could influence species' responses to ecological traps, potentially leading to disparities in trap exposure and severity.

Finally, our model follows the principles of optimal foraging theory, which suggests that individuals make foraging decisions aimed at maximizing their fitness. Decisions about when and where to move are influenced by both hunger and previous foraging success. A valuable enhancement would be to incorporate trade-offs into these decisions (Railsback, 2022), such as those between hunger and fear, or by using more direct fitness measures, including growth, survival, reproduction, and risk avoidance. Incorporating fear, in general terms, is expected to increase species resilience. However, how fear emerges in response to the accumulated experiences of different life history strategies and its population-level consequences remain intriguing avenues for future research.

4.5. Management implications

Our study suggests that compensatory trap models could be essential for understanding and predicting the impacts of anthropogenic food subsidies—such as crops, dumps, restaurants, offal, and fisheries discards—on scavenger species (Munstermann et al., 2022; Oro et al., 2013). These subsidies often come with major fitness costs, including increased risks of poisoning, pathogen infection (e.g., in

birds: Becker et al., 2015), interference competition (e.g., in sharks: Semeniuk and Rothley, 2008), predation (e.g., in mammals and birds, Morris, 2005; Rodewald et al., 2011), hunting (e.g., mammals, Simon and Fortin, 2020), and incidental mortality (e.g., in seabirds, turtles, marine mammals and elasmobranchs: Lewison et al., 2014)

Ecological trap models have evolved from basic source-sink frameworks to realistic IBMs that incorporate habitat selection, individual learning or adaptive capacities, local interactions (both spatial and network-based), and dynamic, heterogeneous environments. These models are increasingly applied in terrestrial ecosystems to assess ecological traps, providing valuable insights for management and conservation strategies (Sánchez-Clavijo et al., 2016; Simon and Fortin, 2020). In contrast, the application of such models in marine ecosystems has remained notably absent, despite growing empirical evidence of their importance (Swearer et al., 2021). For example, in seabird-fishery interactions, ecological trap frameworks have primarily focused on fitness declines driven by low-quality food sources, as described by the "junk food hypothesis" (Grémillet et al., 2008). Our findings, alongside existing evidence, emphasize the urgent need to recognize compensatory traps as a unintended consequence of fisheries activities, particularly when they are considered in the long term. These traps should be regarded as a cornerstone for advancing ecosystem-based fisheries management (EBFM) (Pikitch et al., 2004).

Integrating compensatory trap models into EBFM frameworks could substantially enhance conservation and management outcomes. These models could complement current population risk assessments—such as those endorsed by ACAP (Agreement on the Conservation of Albatrosses and Petrels)—which often overlook the broader role of trophic subsidies (i.e., interactive effect with the bycatch). Moreover, they could help establish clear, measurable management objectives and define fishery-specific thresholds. Compensatory trap models could be parametrized from seabird movement

and behavior (www.seabirdtracking.org, Carneiro et al., 2024), metabolism (Dunn et al., 2018; Sibly et al., 2013), demography and fisheries data (e.g., bycatch and energy from discards) gathered through onboard observer programs. These models could play a vital role in evaluating management strategies for bycatch and discards, helping to prevent and mitigate ecological traps (by detecting thresholds) while assessing situations where discards might positively influence reproductive traits and population persistence. For instance, Genovart et al., (2016) demonstrated how bycatch poses an unsustainable threat to the Balearic shearwater population and suggested that a discard ban could paradoxically accelerate the species' decline.

5. Conclusion

We developed a compensatory ecological trap model involving a trade-off between recruitment and survival. Our model reveals a critical interaction between trap subsidies and mortality, with distinct thresholds for species depending on their position across the slow-fast life history continuum. These thresholds mark the transition from the beneficial effects of trophic subsidies to negative synergistic effects with mortality, driven by increased effective mortality associated with greater habitat preference. Our findings showed that, under similar conditions (e.g., comparable metabolism and behavior), slow species are more vulnerable to extinction in compensatory traps—1.4 times more vulnerable than intermediate species and 4.5 times more vulnerable than fast species—while fast species demonstrate greater resilience and a higher potential for population growth. These results support and extend previous predictions about ecological traps, highlighting the need to broaden the conceptual framework to account for a wider range of fitness trade-offs. By deepening our understanding of these dynamics, we can better predict how ecological traps impact populations of species with varying life history traits and their potential to shape biodiversity by selectively pruning the tree of life. Based on our results, we propose that compensatory traps may play a fundamental role

652 in driving interactions between wildlife and human-derived trophic subsidies, such as those between
653 seabirds and fisheries. In these contexts, compensatory traps offer a critical conceptual and predictive
654 framework for advancing EBFM, ultimately improving the effectiveness of conservation and
655 management strategies.

656

657

658

659

660

661

662

663

664

665

666

667

668

669

Acknowledgments: CA thanks the funding received from the National Agency for Research and Development (ANID) / Scholarship Program / National Doctorate 2020- 21201056

689 **Tables**

690 Table 1. List of parameters used in the model.

Abbreviation	Description (units)	Values
Life cycle parameters		
β_hunger	Hunger (KJ)	1000
β_basal	Basal energy expenditure (KJ)	β_hunger/3.5
β_loss	Energy loss from movement (KJ)	β_basal /8
β_radius	Radius of movement (cells)	5
β_dire, k_dire	Parameters of movement directionality	β_dire=-0.2, k_dire=30°
β_holling	Constant in functional consumption	β_hunger*0.9
β_reproduction	Energy of reproduction (satiated steps)	450 (~52% non-breeding season)
β_supply	Energy cost of chick production and supply (KJ)	β_hunger*0.1
β_fledge	Number of provisioning events	110 (~once a day)
β_starvation	Starvation mortality (days without food)	10
β_constant	Annual constant mortality	1%
β_memory	Number of cells birds remember	30
Life history parameters		
β_clutch	Clutch size (number of offspring)	Slow= 1, intermediate= 2, fast= 3
β_firstbreed	Age of first reproduction (years)	Slow= 9, intermediate= 4, fast= 3
β_min, β_max	Age-mortality (min-max exponential function)	Slow= 5-25%, intermediate= 15-35%, fast= 20-40%

β_senescence	Max age (years)	Slow= 40, intermediate = 25, fast= 20
Environmental parameters		
β_mu, β_sigma, β_nu	Parameters of the energy raster (ZINBI)	β_mu = 2, β_sigma = 0.5, β_nu= 0.2
β_food	Food multiplicator	3500
β_replenishment	Energy replenishment time (steps)	12
Trap parameters		
β_proportion	Proportion of trapped area	15%
β_where	Where the trap occurs (energy raster decile)	9 (except the random trap scenario)
β_subsidy	Subsidized energy per cell (KJ)	Low= 500, medium= 1500, high=3500
β_lethality	Probability of mortality in trap-cells	Low=2.50E-04, medium= 5.00E-04, high= 7.50E-04

Figures

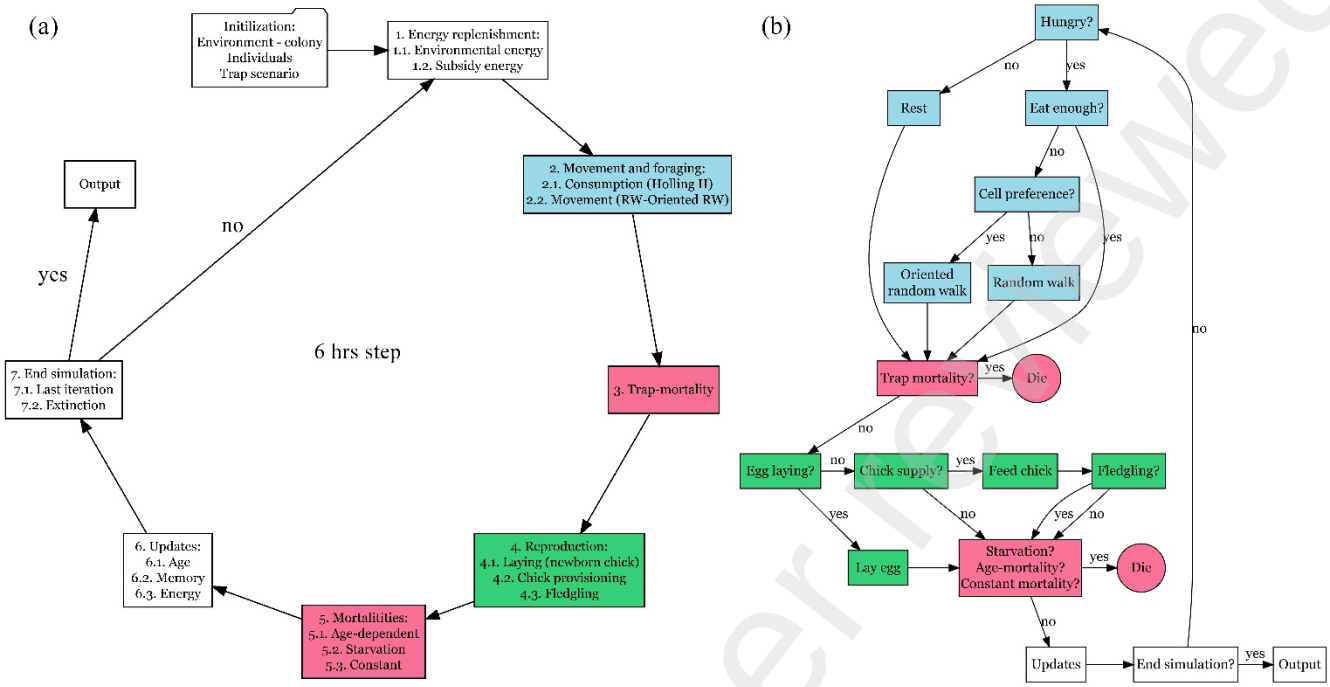

Figure 1. Overview of the program structure (a) and model components (b). (a) illustrates the sequence of the seven sub-models within the program, while (b) provides a detailed view of the algorithms for the Movement and Foraging, Reproduction, and Mortalities sub-models, depicting the decision-making and actions processes by individuals throughout their life cycle. The Reproduction sub-model (in green) is executed only during the reproductive season.

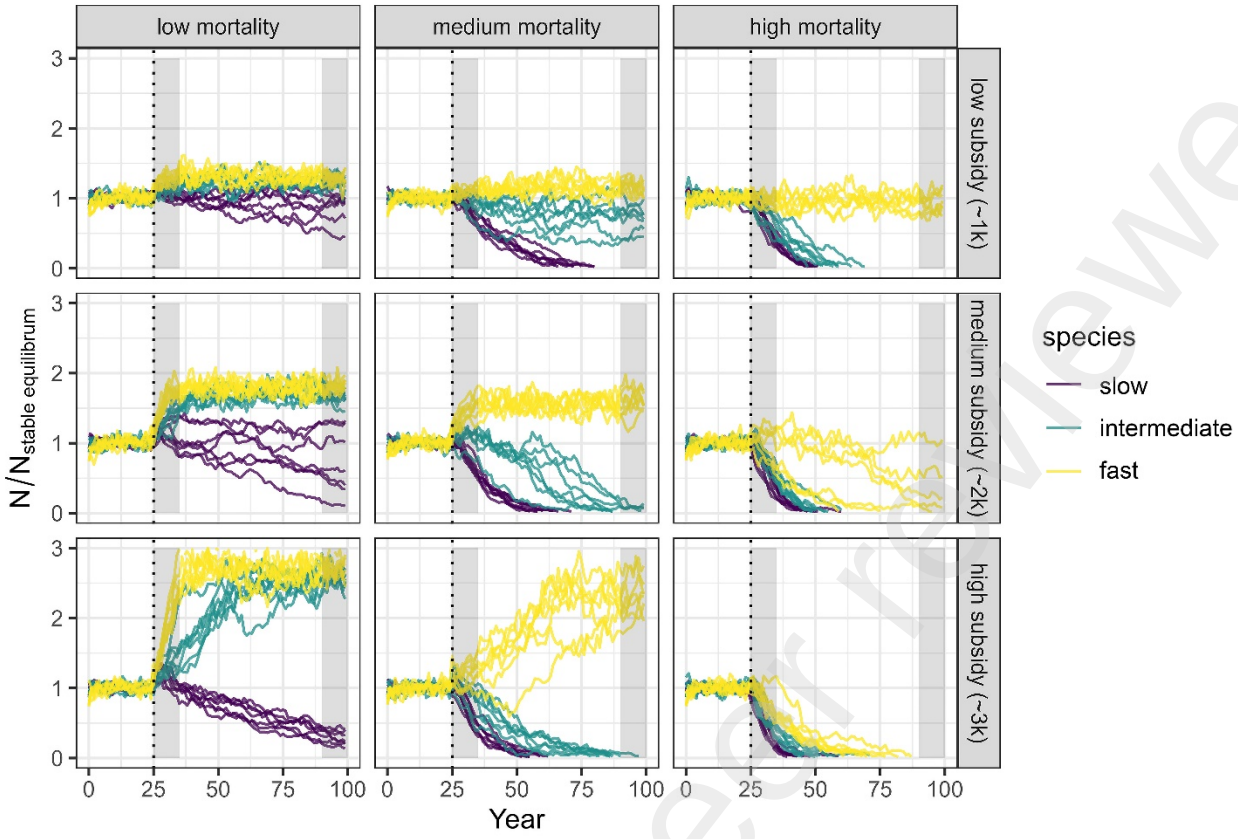

711

712 Figure 2. Population responses of species with different life histories—slow (albatross), intermediate
713 (gull), and fast (cormorant)—to a compensatory ecological trap involving a demographic trade-off
714 between decreased survival and increased recruitment due to trophic subsidies (n = 189 models; 3 life
715 histories × 3 subsidy levels × 3 mortality levels × 7 replicates). Population sizes are standardized to the
716 steady-state size observed in the first 24 years under control conditions. The ecological trap (base
717 scenario) is introduced continuously from year 25 onward (indicated by the dashed line). Gray bars
718 highlight short- and long-term responses (see Figure 3).

719

720

721

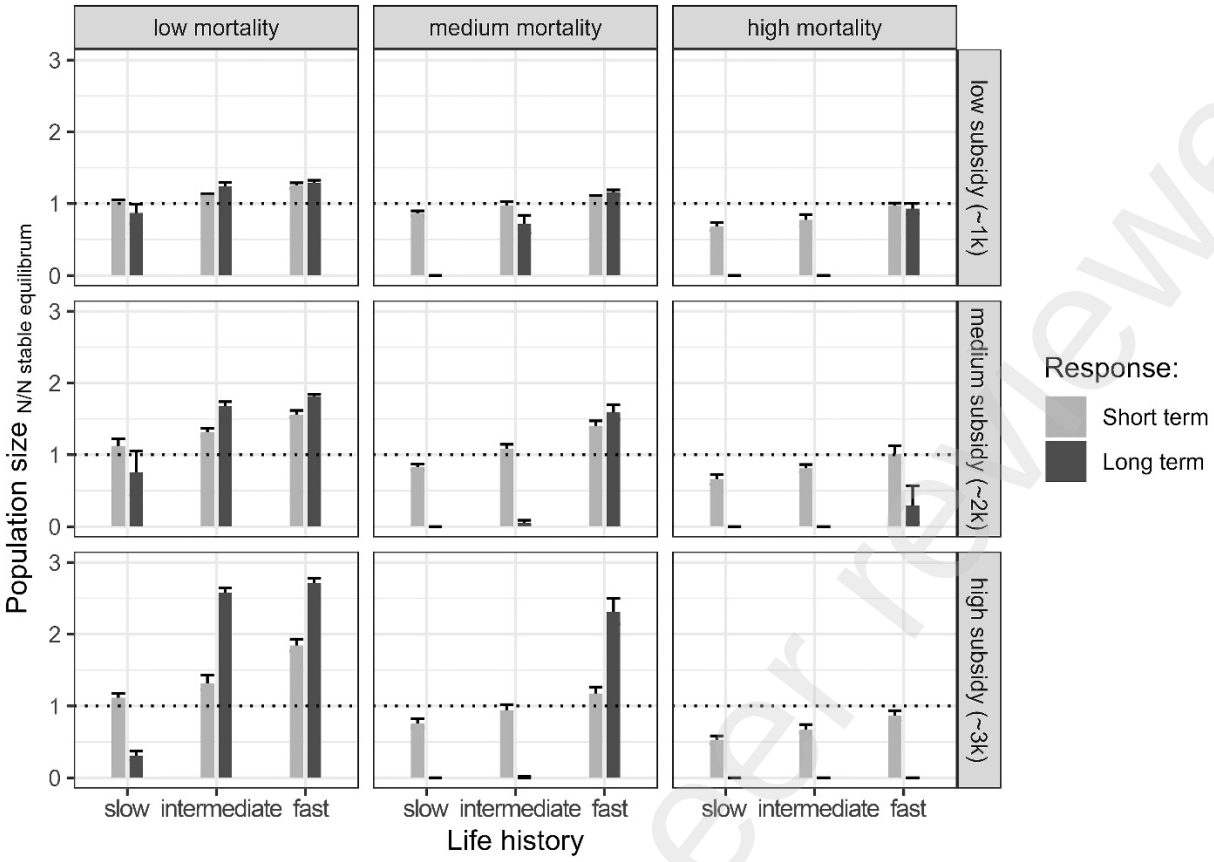

722

723 Figure 3. Short- and long-term population responses (mean ± bootstrapped 95% confidence interval) of
724 species with varying life histories—slow (albatross), intermediate (gull), and fast (cormorant)—to a
725 compensatory ecological trap involving a demographic trade-off between decreased survival and
726 increased recruitment due to trophic subsidies (n = 189 models; 3 life histories × 3 subsidy levels × 3
727 mortality levels × 7 replicates). Population sizes are standardized to the steady-state size observed in
728 the first 24 years under control conditions.

729

730

731

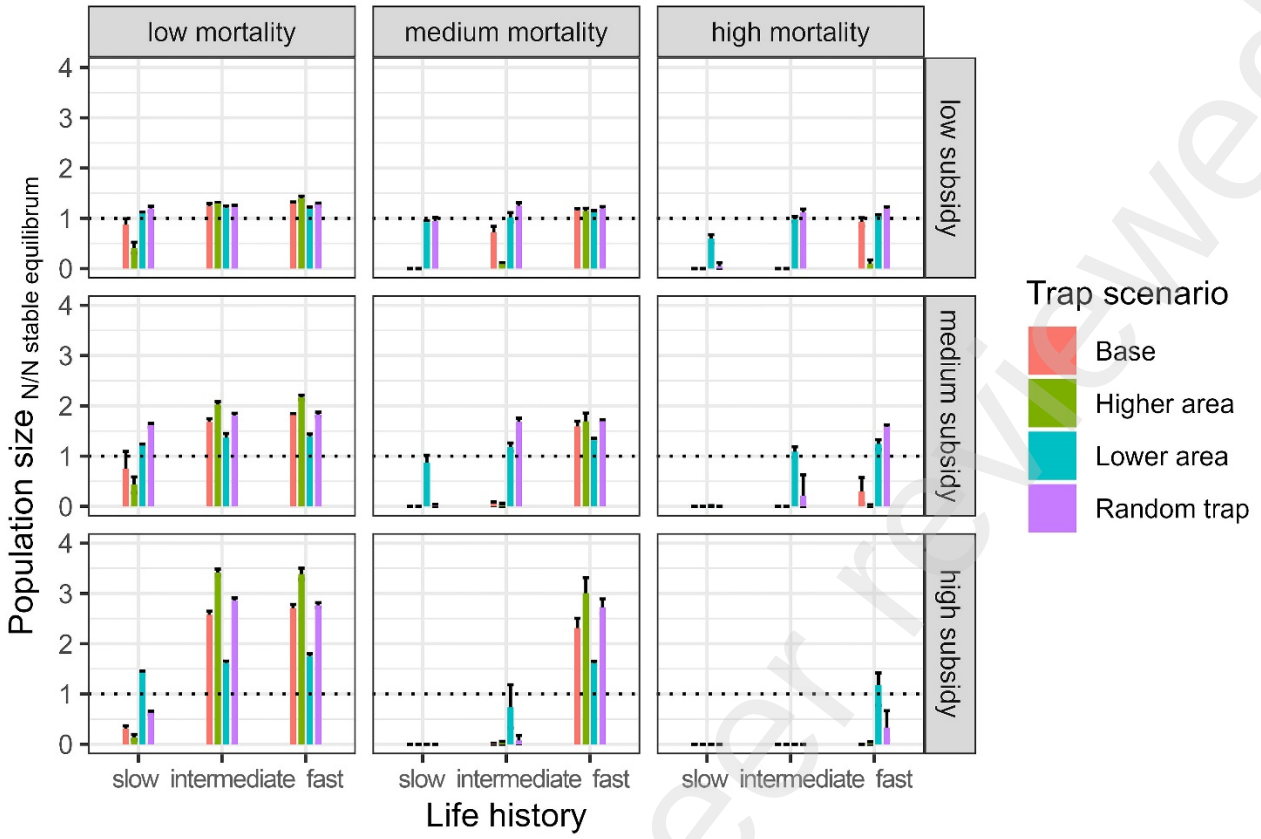

732

733 Figure 4. Long-term population responses (mean ± bootstrapped 95% confidence interval) of species
734 with varying life histories—slow (albatross), intermediate (gull), and fast (cormorant)—to the base
735 scenario of the compensatory trap, a larger-area scenario (25% of the habitat), a smaller-area scenario
736 (5% of the habitat), and a scenario in which the trap occurred randomly throughout the habitat.
737 Population sizes are standardized to the steady-state size observed during the first 24 years under
738 control conditions.

739

740

741

742

References

Abraham, E.R., Pierre, J.P., Middleton, D.A.J., Cleal, J., Walker, N.A., Waugh, S.M., 2009. Effectiveness of fish waste management strategies in reducing seabird attendance at a trawl vessel. Fish Res 95, 210–219. https://doi.org/10.1016/j.fishres.2008.08.014

Barrett, T., Dowle, M., Srinivasan, A., Gorecki, J., Chirico, M., Hocking, T., Schwendinger, B., 2024. data.table: Extension of `data.frame`.

Battin, J., 2004. When Good Animals Love Bad Habitats: Ecological Traps and the Conservation of Animal populations. Conservation Biology 18, 1482–1491.

Bauduin, S., McIntire, E.J.B., Chubaty, A.M., 2019. NetLogoR: a package to build and run spatially explicit agent-based models in R. Ecography 42, 1841–1849. https://doi.org/10.1111/ecog.04516

Becker, D.J., Streicker, D.G., Altizer, S., 2015. Linking anthropogenic resources to wildlife-pathogen dynamics: A review and meta-analysis. Ecol Lett. https://doi.org/10.1111/ele.12428

Bicknell, A.W.J., Oro, D., Camphuysen, K.C.J., Votier, S.C., 2013. Potential consequences of discard reform for seabird communities. Journal of Applied Ecology 50, 649–658. https://doi.org/10.1111/1365-2664.12072

Brown, J.H., 2004. Toward a metabolic theory of ecology. Ecology 85, 1771–1789.

Capdevila, P., Beger, M., Blomberg, S.P., Hereu, B., Linares, C., Salguero-Gómez, R., 2020. Longevity, body dimension and reproductive mode drive differences in aquatic versus terrestrial life-history strategies. Funct Ecol 34, 1613–1625. https://doi.org/10.1111/1365-2435.13604

Capdevila, P., Stott, I., Cant, J., Beger, M., Rowlands, G., Grace, M., Salguero-Gómez, R., 2022. Life history mediates the trade-offs among different components of demographic resilience. Ecol Lett 25, 1566–1579. https://doi.org/10.1111/ele.14004

Carmona, C.P., Tamme, R., Pärtel, M., De Bello, F., Brosse, S., Capdevila, P., González-M, R., González-Suárez, M., Salguero-Gómez, R., Vásquez-Valderrama, M., Toussaint, A., 2021. Erosion of global functional diversity across the tree of life. Sci. Adv 7.

Carneiro, A.P.B., Dias, M.P., Clark, B.L., Pearmain, E.J., Handley, J., Hodgson, A.R., Croxall, J.P., Phillips, R.A., Oppel, S., Morten, J.M., Lascelles, B., Cunningham, C., Taylor, F.E., Miller, M.G.R., Taylor, P.R., Bernard, A., Grémillet, D., Davies, T.E., 2024. The BirdLife Seabird Tracking Database: 20 years of collaboration for marine conservation. Biol Conserv 299. https://doi.org/10.1016/j.biocon.2024.110813

Charnov, E., 1976. Optimal foraging: The marginal value theorem. Theor Popul Biol 9, 129–136.

Clark, T.J., Luis, A.D., 2020. Nonlinear population dynamics are ubiquitous in animals. Nat Ecol Evol 4, 75–81. https://doi.org/10.1038/s41559-019-1052-6

Cleeland, J.B., Pardo, D., Raymond, B., Tuck, G.N., McMahon, C.R., Phillips, R.A., Alderman, R., Lea, M.A., Hindell, M.A., 2021. Disentangling the Influence of Three Major Threats on the Demography of an Albatross Community. Front Mar Sci 8. https://doi.org/10.3389/fmars.2021.578144

Cooke, R.S.C., Eigenbrod, F., Bates, A.E., 2019. Projected losses of global mammal and bird ecological strategies. Nat Commun 10. https://doi.org/10.1038/s41467-019-10284-z

779 Cooney, C.R., Sheard, C., Clark, A.D., Healy, S.D., Liker, A., Street, S.E., Troisi, C.A., Thomas, G.H., Székely, T.,
780 Hemmings, N., Wright, A.E., 2020. Ecology and allometry predict the evolution of avian developmental
781 durations. Nat Commun 11. https://doi.org/10.1038/s41467-020-16257-x

782 Delibes, M., Gaona, P., Ferreras, P., 2001. Effects of an Attractive Sink Leading into Maladaptive Habitat
783 Selection. Am Nat 158, 1–44.

784 Dias, M.P., Martin, R., Pearmain, E.J., Burfield, I.J., Small, C., Phillips, R.A., Yates, O., Lascelles, B., Borboroglu,
785 P.G., Croxall, J.P., 2019. Threats to seabirds: A global assessment. Biol Conserv 237, 525–537.
786 https://doi.org/10.1016/j.biocon.2019.06.033

787 Donovan, T.M., Thompson, F.R., 2001. Modeling The Ecological Trap Hypothesis: A Habitat and Demographic
788 Analysis for Migrant Songbirds. Ecological Applications 11, 871–882. https://doi.org/10.2307/3061122

789 Dunn, R.E., White, C.R., Green, J.A., 2018. A model to estimate seabird field metabolic rates. Biol Lett 14.
790 https://doi.org/10.1098/rsbl.2018.0190

791 Dwernychuk, L.W., Boag, D.A., 1972. Ducks nesting in association with gulls-an ecological trap? Can J Zool 50,
792 559–563.

793 Fletcher, R.J., Orrock, J.L., Robertson, B.A., 2012a. How the type of anthropogenic change alters the
794 consequences of ecological traps. Proceedings of the Royal Society B: Biological Sciences 279, 2546–2552.
795 https://doi.org/10.1098/rspb.2011.0139

796 Fletcher, R.J., Orrock, J.L., Robertson, B.A., 2012b. How the type of anthropogenic change alters the
797 consequences of ecological traps. Proceedings of the Royal Society B 279, 2546–2552.
798 https://doi.org/10.1098/rspb.2011.0139

799 Gaillard, J.M., Lemaître, J.F., Berger, V., Bonenfant, C., Devillard, S., Douhard, M., Gamelon, M., Plard, F.,
800 Lebreton, J.D., 2016. Life Histories, Axes of Variation in. Encyclopedia of Evolutionary Biology.
801 https://doi.org/10.1016/B978-0-12-800049-6.00085-8

802 Garthe, S., Camphuysen, K., Furness, R.W., 1996. Amounts of discards by commercial fisheries and their
803 significance as food for seabirds in the North Sea. Mar Ecol Prog Ser 136, 1–11.
804 https://doi.org/10.3354/meps136001

805 Gates, J.E., Gysel, L.W., 1978. Avian nest dispersion and fledging success in field-forest ecotones. Ecology 59,
806 871–883.

807 Genovart, M., Arcos, J.M., Alvarez, D., McMinn, M., Meier, R., Wynn, R.B., Guilford, T., Oro, D., Álvarez, D.,
808 McMinn, M., Meier, R., B. Wynn, R., Guilford, T., Oro, D., 2016. Demography of the critically endangered
809 Balearic shearwater: the impact of fisheries and time to extinction. Journal of Applied Ecology 53, 1158–
810 1168. https://doi.org/10.1111/1365-2664.12622

811 Genovart, M., Doak, D.F., Igual, J.M., Sponza, S., Kralj, J., Oro, D., 2017. Varying demographic impacts of
812 different fisheries on three Mediterranean seabird species. Glob Chang Biol 23, 3012–3029.
813 https://doi.org/10.1111/gcb.13670

814 Gilman, E., Perez Roda, A., Huntington, T., Kennelly, S.J., Suuronen, P., Chaloupka, M., Medley, P.A.H., 2020.
815 Benchmarking global fisheries discards. Sci Rep 10. https://doi.org/10.1038/s41598-020-71021-x

Grémillet, D., Pichegru, L., Kuntz, G., Woakes, A.G., Wilkinson, S., Crawford, R.J.M., Ryan, P.G., 2008. A junk-food hypothesis for gannets feeding on fishery waste. Proceedings of the Royal Society B: Biological Sciences 275, 1149–1156. https://doi.org/10.1098/rspb.2007.1763

Grimm, V., Berger, U., Bastiansen, F., Eliassen, S., Ginot, V., Giske, J., Goss-Custard, J., Grand, T., Heinz, S.K., Huse, G., Huth, A., Jepsen, J.U., Jørgensen, C., Mooij, W.M., Müller, B., Pe'er, G., Piou, C., Railsback, S.F., Robbins, A.M., Robbins, M.M., Rossmanith, E., Rüger, N., Strand, E., Souissi, S., Stillman, R.A., Vabø, R., Visser, U., DeAngelis, D.L., 2006. A standard protocol for describing individual-based and agent-based models. Ecol Modell 198, 115–126. https://doi.org/10.1016/j.ecolmodel.2006.04.023

Grimm, V., Railsback, S.F., 2005. Individual-based modeling and ecology. Princeton university press, princeton, New Jersey.

Hale, R., Swearer, S.E., 2016. Ecological traps: Current evidence and future directions. Proceedings of the Royal Society B: Biological Sciences 283. https://doi.org/10.1098/rspb.2015.2647

Hale, R., Treml, E.A., Swearer, S.E., 2015. Evaluating the metapopulation consequences of ecological traps. Proceedings of the Royal Society B: Biological Sciences 282. https://doi.org/10.1098/rspb.2014.2930

Hatton, I.A., Dobson, A.P., Storch, D., Galbraith, E.D., Loreau, M., 2019. Linking scaling laws across eukaryotes. Proc Natl Acad Sci U S A 116, 21616–21622. https://doi.org/10.1073/pnas.1900492116

Heppell, S.S., Caswell, H., Crowder, L.B., 2000. Life histories and elasticity patterns: Perturbation analysis for species with minimal demographic data. Ecology 81, 654–665. https://doi.org/10.1890/0012-9658(2000)081[0654:LHAEPP]2.0.CO;2

Herrando-Pèrez, S., Delean, S., Brook, B.W., Bradshaw, C.J.A., 2012. Strength of density feedback in census data increases from slow to fast life histories. Ecol Evol 2, 1922–1934. https://doi.org/10.1002/ece3.298

Holling, C.S., 1959. Some characteristics of simple types of predation and parasitism. Can Entomol 91, 385–398.

Karpouzi, V.S., Watson, R., Pauly, D., 2007. Modelling and mapping resource overlap between seabirds and fisheries on a global scale: A preliminary assessment. Mar Ecol Prog Ser 343, 87–99. https://doi.org/10.3354/meps06860

Kokko, H., Sutherland, W.J., 2001. Ecological traps in changing environments: Ecological and evolutionary consequences of a behaviourally mediated Allee effect. Evol Ecol Res 3, 537–551.

Kristan, William B, Kristan, I., Kristan, W B, 2003. The role of habitat selection behavior in population dynamics: source-sink systems and ecological traps. Oikos 103, 457–468.

Langlois Lopez, S., Bond, A.L., O'Hanlon, N.J., Wilson, J.M., Vitz, A., Mostello, C.S., Hamilton, F., Rail, J.F., Welch, L., Boettcher, R., Wilhelm, S.I., Anker-Nilssen, T., Daunt, F., Masden, E., 2023. Global population and conservation status of the Great Black-backed Gull Larus marinus. Bird Conserv Int 33. https://doi.org/10.1017/S0959270922000181

Lewison, R.L., Crowder, L.B., Wallace, B.P., Moore, J.E., Cox, T., Zydelis, R., McDonald, S., DiMatteo, A., Dunn, D.C., Kot, C.Y., Bjorkland, R., Kelez, S., Soykan, C., Stewart, K.R., Sims, M., Boustany, A., Read, A.J., Halpin, P., Nichols, W.J., Safina, C., 2014. Global patterns of marine mammal, seabird, and sea turtle bycatch reveal taxa-specific and cumulative megafauna hotspots. Proceedings of the National Academy of Sciences 111, 5271–5276. https://doi.org/10.1073/pnas.1318960111

Morris, D.W., 2005. Paradoxical avoidance of enriched habitats: Have we failed to appreciate omnivores? Ecology 86, 2568–2577. https://doi.org/10.1890/04-0909

Munch, S.B., Snover, M.L., Watters, G.M., Mangel, M., 2005. A unified treatment of top-down and bottom-up control of reproduction in populations. Ecol Lett 8, 691–695. https://doi.org/10.1111/j.1461-0248.2005.00766.x

Munstermann, M.J., Heim, N.A., McCauley, D.J., Payne, J.L., Upham, N.S., Wang, S.C., Knope, M.L., 2022. A global ecological signal of extinction risk in terrestrial vertebrates. Conservation Biology 36. https://doi.org/10.1111/cobi.13852

Oro, D., 1996. Effects of trawler discard availability on egg laying and breeding success in the lesser black-backed gull Larus fuscus in the western Mediterranean. Mar Ecol Prog Ser 132, 43–46.

Oro, D., Bosch, M., Ruiz, X., 1995. Effects of a trawling moratorium on the breeding success of the Yellow-legged Gull Larus cachinnans. Ibis 137, 547–549.

Oro, D., Genovart, M., Tavecchia, G., Fowler, M.S., Martínez-Abraín, A., 2013. Ecological and evolutionary implications of food subsidies from humans. Ecol Lett 16, 1501–1514. https://doi.org/10.1111/ele.12187

Oro, D., Jover, L., Ruiz, X., 1996. Influence of trawling activity on the breeding ecology of a threatened seabird, Audouin\'s gull Larus audouinii. Mar Ecol Prog Ser 139, 19–29.

Pardo, D., Forcada, J., Wood, A.G., Tuck, G.N., Ireland, L., Pradel, R., Croxall, J.P., Phillips, R.A., 2017. Additive effects of climate and fisheries drive ongoing declines in multiple albatross species. Proceedings of the National Academy of Sciences 114, E10829–E10837. https://doi.org/10.1073/pnas.1618819114

Peters, R.H., 1983. The Ecological Implications of Body Size, The Ecological Implications of Body Size. Cambridge University Press. https://doi.org/10.1017/cbo9780511608551

Pierre, J.P., Abraham, E.R., Richard, Y., Cleal, J., Middleton, D.A.J., 2012. Controlling trawler waste discharge to reduce seabird mortality. Fish Res 131, 30–38. https://doi.org/10.1016/j.fishres.2012.07.005

Pikitch, E.K., Santora, C., Babcock, E.A., Bakun, A., Bonfil, R., Conover, D.O., Dayton, P., Doukakis, P., Fluharty, D., Heneman, B., 2004. Ecosystem-based fishery management. Science (1979) 305, 346–347.

R Core Team, 2023. R: A language and environment for statistical computing.

Railsback, S.F., 2022. Suboptimal foraging theory: How inaccurate predictions and approximations can make better models of adaptive behavior. Ecology 103. https://doi.org/10.1002/ecy.3721

Richards, C., Cooke, R., Bowler, D.E., Boerder, K., Bates, A.E., 2024. Bycatch-threatened seabirds disproportionally contribute to community trait composition across the world. Glob Ecol Conserv 49. https://doi.org/10.1016/j.gecco.2023.e02792

Richards, C., Cooke, R.S.C.C., Bates, A.E., 2021. Biological traits of seabirds predict extinction risk and vulnerability to anthropogenic threats. Global Ecology and Biogeography 30, 973–986. https://doi.org/10.1111/geb.13279

Robert Burger, J., Hou, C., A. S. Hall, C., Brown, J.H., 2021. Universal rules of life: metabolic rates, biological times and the equal fitness paradigm. Ecol Lett. https://doi.org/10.1111/ele.13715

Robertson, B.A., Blumstein, D.T., 2019. How to disarm an evolutionary trap. Conserv Sci Pract e116. https://doi.org/10.1111/csp2.116

892 Robertson, B.A., Rehage, J.S., Sih, A., 2013. Ecological novelty and the emergence of evolutionary traps. Trends
893 Ecol Evol 28, 552–560. https://doi.org/10.1016/j.tree.2013.04.004

894 Rodewald, A.D., Kearns, L.J., Shustack, D.P., 2011. Anthropogenic resource subsidies decouple predator-prey
895 relationships. Ecological Applications 21, 936–943.

896 Rogers, T.L., Johnson, B.J., Munch, S.B., 2022. Chaos is not rare in natural ecosystems. Nat Ecol Evol 6, 1105–
897 1111.

898 Rolland, V., Barbraud, C., Weimerskirch, H., 2009. Assessing the impact of fisheries, climate and disease on the
899 dynamics of the Indian yellow-nosed Albatross. Biol Conserv 142, 1084–1095.
900 https://doi.org/10.1016/j.biocon.2008.12.030

901 Rolland, V., Barbraud, C., Weimerskirch, H., 2008. Combined effects of fisheries and climate on a migratory
902 long-lived marine predator. Journal of Applied Ecology 45, 4–13. https://doi.org/10.1111/j.1365-
903 2664.2007.01360.x

904 Rolland, V., Weimerskirch, H., Barbraud, C., 2010. Relative influence of fisheries and climate on the
905 demography of four albatross species. Glob Chang Biol 16, 1910–1922. https://doi.org/10.1111/j.1365-
906 2486.2009.02070.x

907 Saether, B.-E., 1987. The influence of body weight on the covariation between reproductive traits in European
908 birds. Oikos 48, 79–88.

909 Saether, B.-E., Bakke, Ø., 2000. Avian life history variation and contribution of demographic traits to the
910 population growth rate. Ecology 81, 642–653.

911 Sæther, B.E., Engen, S., Møller, A.P., Weimerskirch, H., Visser, M.E., Fiedler, W., Matthysen, E., Lambrechts,
912 M.M., Badyaev, A., Becker, P.H., Brommer, J.E., Bukacinski, D., Bukacinska, M., Christensen, H., Dickinson,
913 J., Du Feu, C., Gehlbach, F.R., Heg, D., Hötker, H., Merilä, J., Nielsen, J.T., Rendell, W., Robertson, R.J.,
914 Thomson, D.L., Török, J., Van Hecke, P., 2004. Life-history variation predicts the effects of demographic
915 stochasticity on avian population dynamics. American Naturalist 164, 793–802.
916 https://doi.org/10.1086/425371

917 Sánchez-Clavijo, L.M., Hearns, J., Quintana-Ascencio, P.F., 2016. Modeling the effect of habitat selection
918 mechanisms on population responses to landscape structure. Ecol Modell 328, 99–107.
919 https://doi.org/10.1016/j.ecolmodel.2016.03.004

920 Scales, K.L., Hazen, E.L., Jacox, M.G., Castruccio, F., Maxwell, S.M., Lewison, R.L., Bograd, S.J., 2018. Fisheries
921 bycatch risk to marine megafauna is intensified in Lagrangian coherent structures. Proc Natl Acad Sci U S
922 A 115, 7362–7367. https://doi.org/10.1073/pnas.1801270115

923 Schreiber, E.A., Burger, J. (Eds.), 2001. Biology of marine birds, Book. CRS Press, Boca Raton, Florida.
924 https://doi.org/10.1650/0010-5422(2003)105[0392:BR]2.0.CO;2

925 Semeniuk, C.A.D., Rothley, K.D., 2008. Costs of group-living for a normally solitary forager: Effects of
926 provisioning tourism on southern stingrays Dasyatis americana. Mar Ecol Prog Ser 357, 271–282.
927 https://doi.org/10.3354/meps07299

928 Sherley, R.B., Ladd-Jones, H., Garthe, S., Stevenson, O., Votier, S.C., 2019. Scavenger communities and fisheries
929 waste: North Sea discards support 3 million seabirds, 2 million fewer than in 1990. Fish and Fisheries 21,
930 132–145. https://doi.org/10.1111/faf.12422

Sibly, R.M., Grimm, V., Martin, B.T., Johnston, A.S.A., Kulakowska, K., Topping, C.J., Calow, P., Nabe-Nielsen, J., Thorbek, P., Deangelis, D.L., 2013. Representing the acquisition and use of energy by individuals in agent-based models of animal populations. Methods Ecol Evol 4, 151–161. https://doi.org/10.1111/2041-210x.12002

Sibly, R.M., Witt, C.C., Wright, N.A., Venditti, C., Jetz, W., Brown, J.H., 2012. Energetics, lifestyle, and reproduction in birds. Proc Natl Acad Sci U S A 109, 10937–10941. https://doi.org/10.1073/pnas.1206512109

Simon, R.N., Fortin, D., 2020. Crop raiders in an ecological trap: optimal foraging individual-based modeling quantifies the effect of alternate crops. Ecological Applications 30. https://doi.org/10.1002/eap.2111

Stasinopoulos, M., Rigby, R.A., 2023. gamlss.dist: Distributions for Generalized Additive Models for Location Scale and Shape.

Stearns, S.C., 1992. The evolution of life histories. Oxford University Press, New York.

Swearer, S.E., Morris, R.L., Barrett, L.T., Sievers, M., Dempster, T., Hale, R., 2021. An overview of ecological traps in marine ecosystems. Front Ecol Environ 19, 234–242. https://doi.org/10.1002/fee.2322

Tuck, G.N., Thomson, R.B., Barbraud, C., Delord, K., Louzao, M., Herrera, M., Weimerskirch, H., 2015. An integrated assessment model of seabird population dynamics: can individual heterogeneity in susceptibility to fishing explain abundance trends in Crozet wandering albatross? Journal of Applied Ecology 52, 950–959. https://doi.org/10.1111/1365-2664.12462

Véran, S., Gimenez, O., Flint, E., Kendall, W.L., Doherty, P.F., Lebreton, J.D., Veran, S., Gimenez, O., Flint, E., Kendall, W.L., Doherty, P.F., Lebreton, J.D., 2007. Quantifying the impact of longline fisheries on adult survival in the black-footed albatross. Journal of Applied Ecology 44, 942–952. https://doi.org/10.1111/j.1365-2664.2007.01346.x

Votier, S.C., Furness, R.W., Bearhop, S., Crane, J.E., Caldow, R.W.G., Catry, P., Ensor, K., Hamer, K.C., Hudson, A. V., Kalmbach, E., Klomp, N.I., Pfeiffer, S., Phillips, R.A., Prieto, I., Thompson, D.R., 2004. Changes in fisheries discard rates and seabird communities. Nature 427, 727–730. https://doi.org/10.1038/nature02315

Welch, H., Clavelle, T., White, T.D., Cimino, M.A., Kroodsma, D., Hazen, E.L., 2024. Unseen overlap between fishing vessels and top predators in the northeast Pacific. Sci Adv 10, 1.

Wickham, H., François, R., Henry, L., Müller, K., Vaughan, D., 2023. dplyr: A Grammar of Data Manipulation.

Wilhelm, S.I., Rail, J.F., Regular, P.M., Gjerdrum, C., Robertson, G.J., 2016. Large-Scale Changes in Abundance of Breeding Herring Gulls (Larus argentatus) and Great Black-Backed Gulls (Larus marinus) Relative to Reduced Fishing Activities in Southeastern Canada. Waterbirds 39, 136–142. https://doi.org/10.1675/063.039.sp104

Zhou, C., Brothers, N., 2022. Seabird bycatch vulnerability in pelagic longline fisheries based on modelling of a long-term dataset. Bird Conserv Int 32, 259–274. https://doi.org/10.1017/S0959270921000046

Zhou, C., Jiao, Y., Browder, J., 2019. How much do we know about seabird bycatch in pelagic longline fisheries? A simulation study on the potential bias caused by the usually unobserved portion of seabird bycatch. PLoS One 14. https://doi.org/10.1371/journal.pone.0220797

Supplementary material

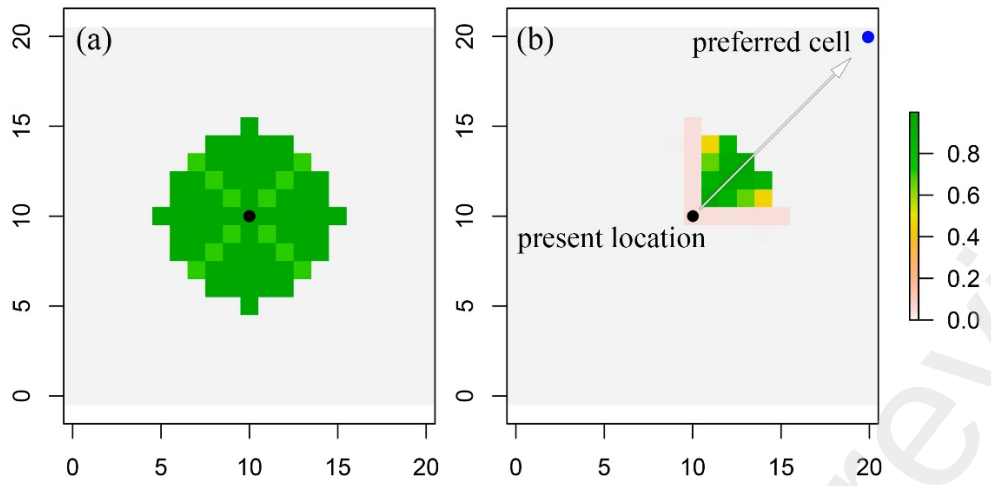

Figure S1. Diagram illustrating how movement probabilities are assigned to cells within the movement radius of an individual (located at the colony, x=10, y=10, in the example), both without (a) and with (b) cell preference. In (a) all cells within the movement radius are assigned equal probability (1), except for diagonal cells, which are penalized (0.7) to maintain isotropic movement. In (b), higher probabilities are assigned to cells in the direction of the preferred cell (blue cell at x = 20, y = 20, in the example). Specifically, the direction from the current cell (x = 10, y = 10) to each surrounding cell is calculated. The same procedure is applied to the preferred cell (x = 20, y = 20). The absolute difference between these direction vectors is computed, and the resulting vector is passed through a logistic function to assign probabilities:

$$\text{Cell probability} = \frac{1}{1 + e^{\text{k\_dire}(\text{direction vectors} - \beta\text{\_dire})}}$$

where β_dire denotes the x value of the function's midpoint and k_dire represents the steepness of the curve. These parameters regulate the degree of stochasticity in movement. Higher values of β_dire and lower values of k increase the probability of selecting cells that deviate from the preferred direction,

thereby introducing a greater degree of stochasticity (see calibration section). The figure illustrates the probabilities assigned using the chosen parameters ($k_{dire} = -0.2$ and $\beta_{dire} = 30°$, see Figure S2).

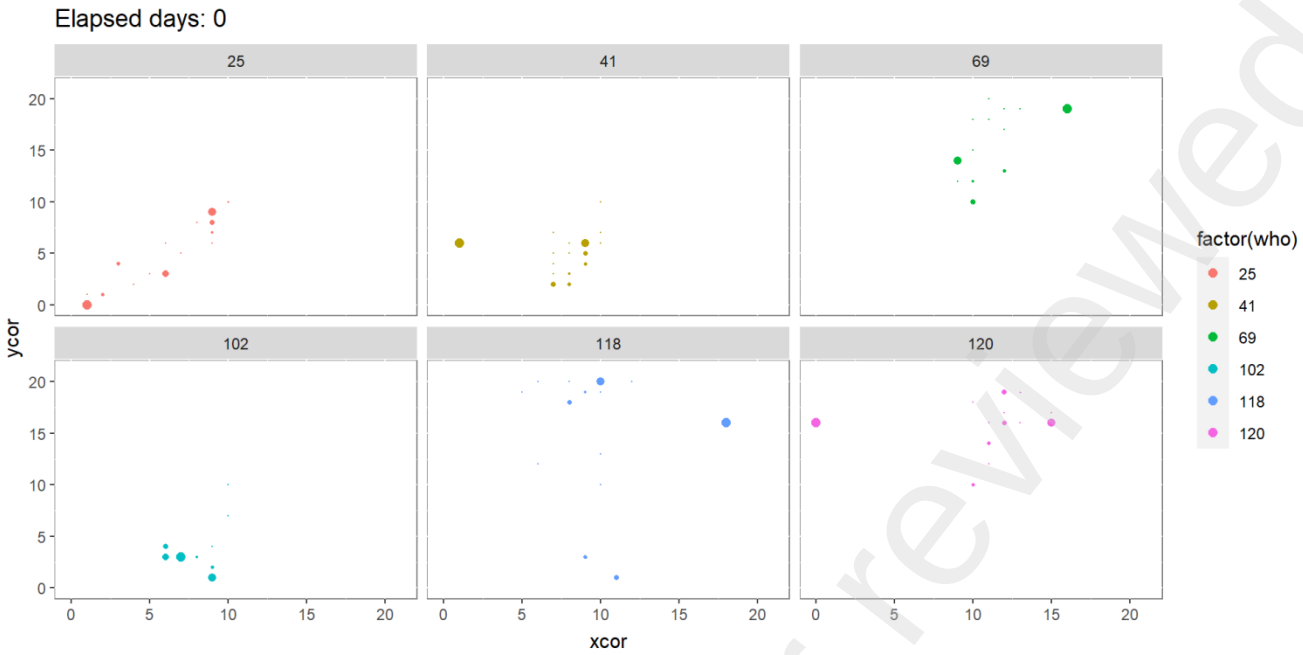

997

998 Figure S2. Animation illustrating the movement of individuals with habitat preference across cells. The
999 annual cycle of six randomly selected individuals in the base model is displayed, with a fade effect
1000 applied to their locations to enhance visualization. On day 219, the reproductive season begins, and the
1001 individuals return to the colony at the center of the raster (x = 10, y = 10) to feed their chick.

1002

1003

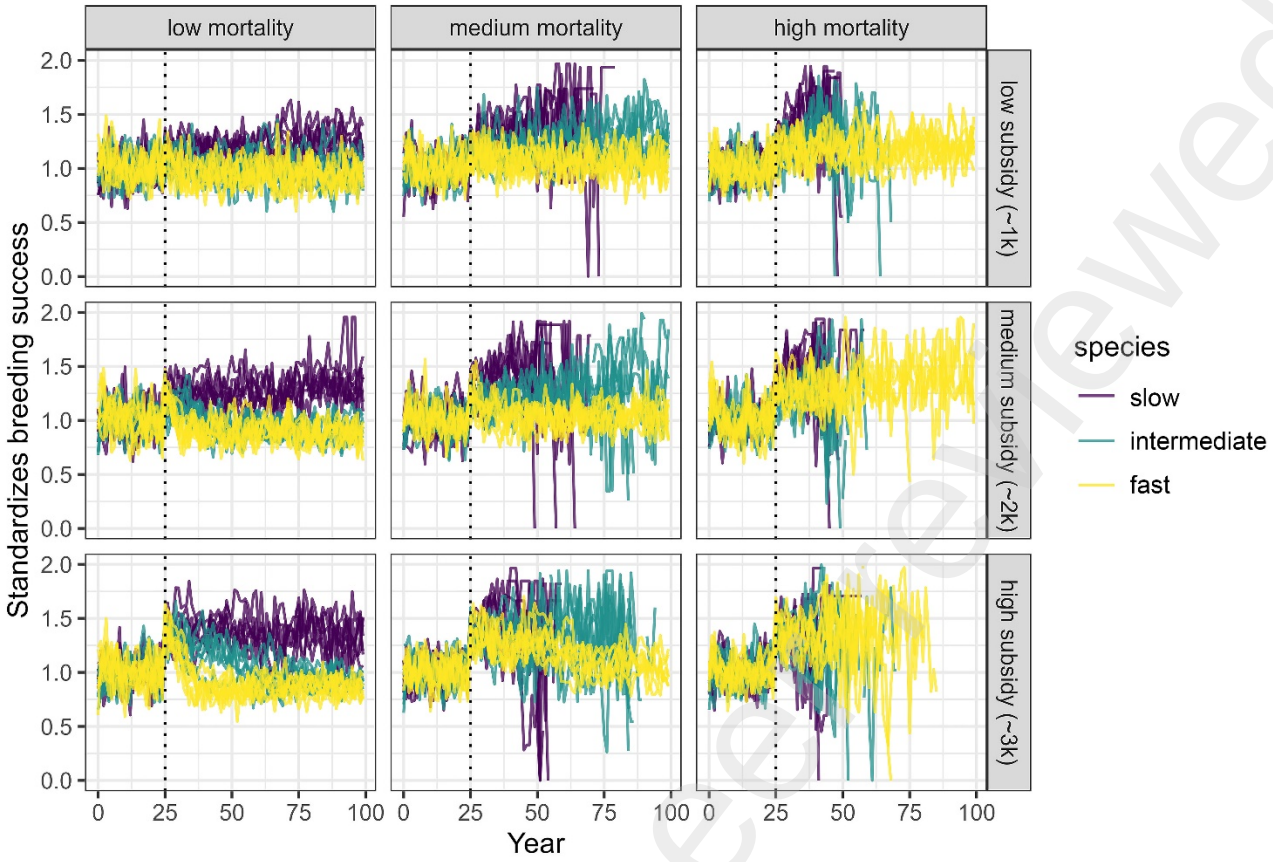

Figure S3. Recruitment of breeders of species with varying life histories—slow (albatross), intermediate (gull), and fast (cormorant)—in the base scenario of the compensatory trap (n = 189 models; 3 life histories × 3 subsidy levels × 3 mortality levels × 7 replicates). The dashed line indicates the start of the trap. The proportion of breeders relative to the total number of birds is shown. Both variables were standardized by the average number observed during the first 24 years under control conditions.

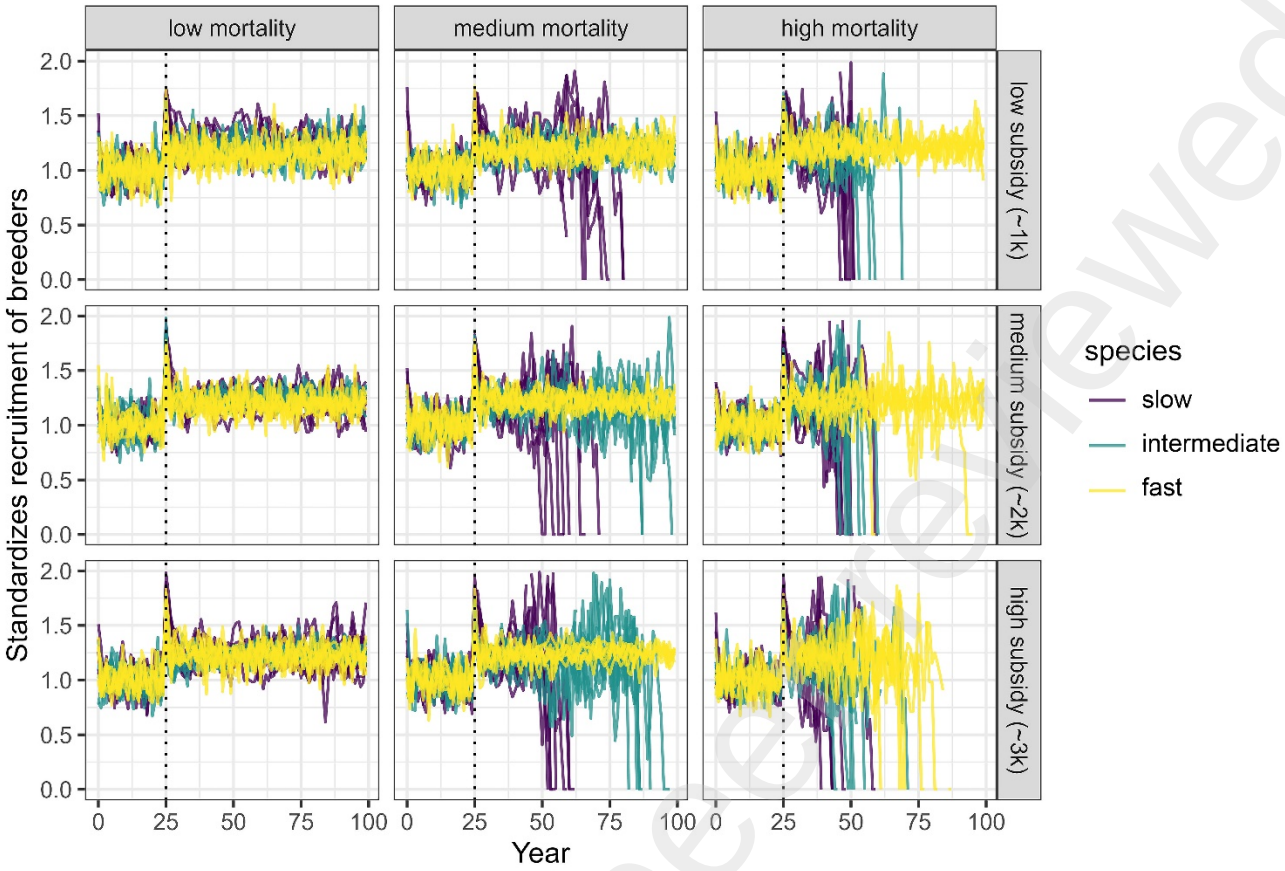

Figure S4. Breeding success of species with varying life histories—slow (albatross), intermediate (gull), and fast (cormorant)—in the base scenario of the compensatory trap (n = 189 models; 3 life histories × 3 subsidy levels × 3 mortality levels × 7 replicates). The dashed line indicates the start of the trap. The proportion of fledged chicks relative to the total number of chicks is shown. Both variables were standardized by the average number observed during the first 24 years under control conditions.

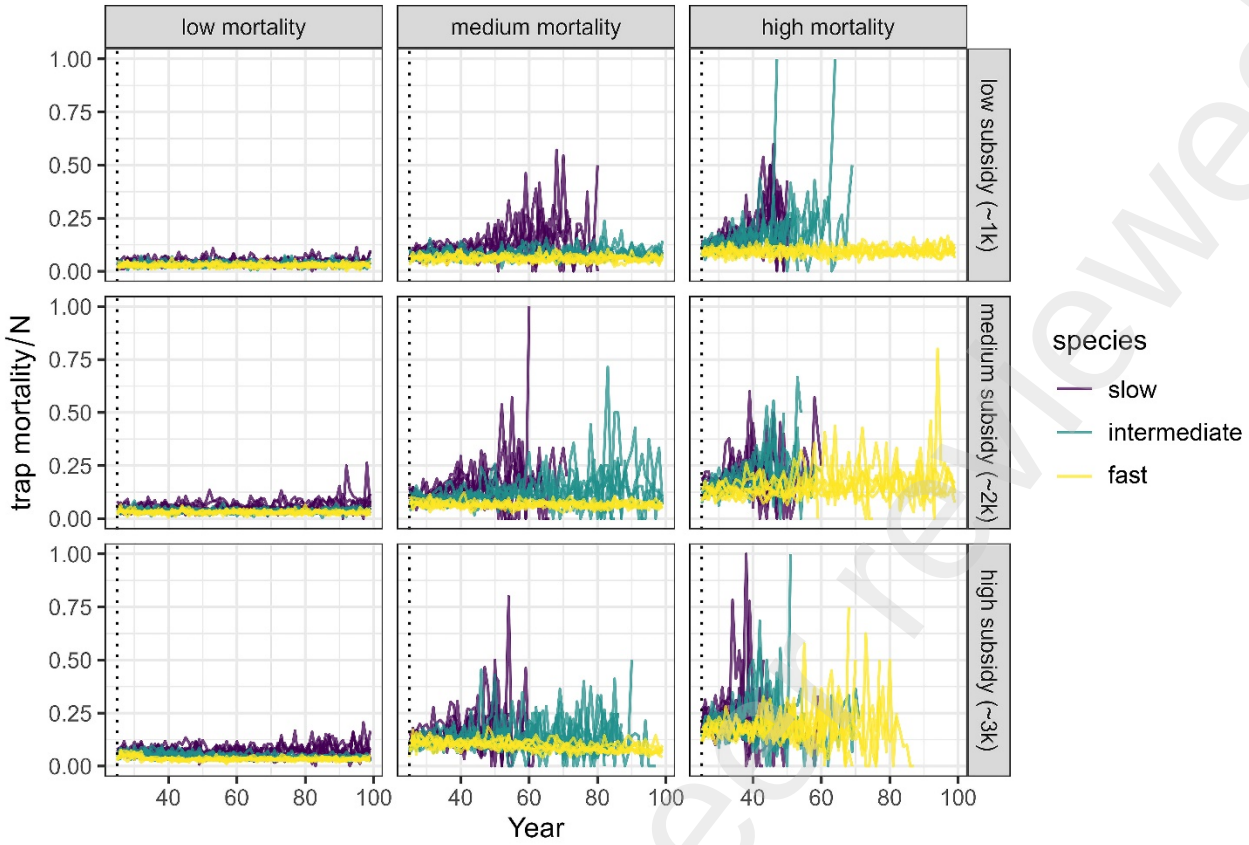

1028

1029 Figure S5. Effective trap mortality of species with varying life histories—slow (albatross), intermediate

1030 (gull), and fast (cormorant)—in the base scenario of the compensatory trap (n = 189 models; 3 life

1031 histories × 3 subsidy levels × 3 mortality levels × 7 replicates).

1032